INTERNATIONAL JOURNAL OF NUMERICAL MODELLING: ELECTRONIC NETWORKS, DEVICES AND FIELDS
Int. J. Numer. Model. 2012; **25**:24–38
Published online 1 March 2011 in Wiley Online Library (wileyonlinelibrary.com). DOI: 10.1002/jnm.809

Accurate macromodeling algorithm for time domain identification of transient port responses

D. Deschrijver*,† and T. Dhaene

Ghent University—IBBT, Department of Information Technology, Sint-Pietersnieuwstraat 41, 9000 Ghent, Belgium

SUMMARY

Orthonormal vector fitting is a robust method for broadband macromodeling of frequency domain responses. The use of orthonormal rational basis functions makes the conditioning of the system equations less sensitive to the initial pole specification when compared with the classical Vector Fitting procedure. This paper presents a time domain generalization of the technique to compute broadband rational macromodels from transient input–output port responses. The efficacy of the approach is illustrated by two numerical examples. Copyright © 2011 John Wiley & Sons, Ltd.

Received 9 July 2010; Revised 25 December 2010; Accepted 1 February 2011

KEY WORDS: time domain; vector fitting; transfer functions; macromodeling; transient responses

1. INTRODUCTION

Reliable synthesis of compact transfer function models is of crucial importance for accurate system-level simulations [1]. The identification of such macromodels from frequency domain measurements or simulations is not a trivial task, even when linear systems are considered [2–5]. Nevertheless, there is an ongoing need for robust and efficient macromodeling techniques that are able to fit resonant frequency responses with a high model order [6]. Vector Fitting (VF) is one of the most popular methods, and has been widely applied in the power systems community [7–10]. Essentially, it minimizes a weighted linear cost function by iteratively relocating a prescribed set of transfer function poles using a Sanathanan–Koerner iteration [11–13]. Numerical ill-conditioning is avoided by using a set of partial fraction basis functions that are based on a well-chosen set of prescribed poles. Such rational basis functions have the advantage that an implicit weighting scheme can be applied, as described in [14]. The implicit weighting was found to give more reliable results if the prescribed poles need to be relocated over long distances, and is therefore preferable.

In [15], it was shown that the method can achieve a higher robustness if the partial fraction basis is replaced by a set of orthonormal rational functions, leading to the orthonormal vector fitting (OVF) technique. Using these orthonormal rational functions, the conditioning of the system equations becomes less sensitive to the initial pole specification, and accurate models can be computed in fewer iterations. This improves the robustness of the method and may lead to a reduction in the overall computation time. It was shown in [16] that orthonormalization can resolve rank deficiency problems if some of the poles become relocated arbitrarily close during

*Correspondence to: D. Deschrijver, Ghent University—IBBT, Department of Information Technology, Sint-Pietersnieuwstraat 41, 9000 Ghent, Belgium.
†E-mail: dirk.deschrijver@intec.ugent.be

the iterations. Such situations occur frequently (although not exclusively) when modeling transfer functions with poles of higher-order multiplicity [17]. The orthonormalization can also lead to more accurate results if exact interpolation problems are solved using Gaussian elimination instead of a rank-revealing QR decomposition [18]. A thorough comparison with the standard partial fraction basis is reported in [14], and it is concluded is that orthonormalization is preferable since it leads to comparable or better results at the expense of a negligible additional computational cost.

The use of these orthonormal basis functions has been succesfully adopted in several applications domains, such as the macromodeling of parameterized frequency responses [19–21], the macromodeling of z-domain responses [22–26], and the modeling and analysis of underground cables and overhead transmission lines [27]. It can be used in conjuction with various passivity enforcement schemes [28–34].

In this paper, a generalization of the OVF approach is presented, which allows the identification of a broadband transfer function based on transient input–output port responses [35]. The idea is based on a time domain implementation of the VF technique, as was shown in [36]. This paper illustrates that the advantages of orthonormalization and time domain identification can be combined, leading to a novel procedure. It is found that this procedure is robust for a wider range of initial pole specifications, and that the additional computational cost is negligible when compared with the standard time domain VF approach. The effectiveness of the proposed technique is illustrated by several numerical examples [37, 38].

2. MODEL REPRESENTATION

The transfer function $R(s)$ is defined as the ratio of a numerator $N(s)$ and denominator $D(s)$

$$R(s) = \frac{N(s)}{D(s)} = \frac{\sum_{p=1}^{P} c_p \Phi_p(s,a)}{\tilde{c}_0 + \sum_{p=1}^{P} \tilde{c}_p \Phi_p(s,a)} \tag{1}$$

Based on the measured or simulated frequency response $\{s_k, H(s_k)\}_{k=0}^{K_s}$ of a microwave component, the coefficients of the macromodel should be estimated in such a way that the least-squares distance between the macromodel and the data is minimized [39]

$$\arg \min_{c_p, \tilde{c}_p} \sum_{k=0}^{K_s} \left| \frac{N(s_k)}{D(s_k)} - H(s_k) \right|^2 \tag{2}$$

In the frequency domain OVF technique, it was shown that a numerically robust procedure is obtained when the numerator and denominator are expanded in a basis of Muntz–Laguerre orthonormal rational functions $\Phi_p(s,a)$ [40]. These basis functions are based on a prescribed set of stable poles $a = \{-a_p\}_{p=1}^{P}$, which are real or occur in complex conjugate pairs. They are chosen according to a heuristic scheme [7].

If $-a_p$ corresponds to a real pole, then the orthonormal basis functions $\Phi_p(s,a)$ are defined as follows:

$$\Phi_p(s,a) = \frac{\sqrt{2\Re e(a_p)}}{s+a_p} \left(\prod_{j=1}^{p-1} \frac{s-a_j^*}{s+a_j} \right) \tag{3}$$

and a linear combination of two basis functions is formed if two poles $-a_p = -a_{p+1}^*$ form a complex conjugate pair

$$\Phi_p(s,a) = \frac{\sqrt{2\Re e(a_p)}(s-|a_p|)}{(s+a_p)(s+a_{p+1})} \prod_{j=1}^{p-1} \frac{s-a_j^*}{s+a_j} \tag{4}$$

$$\Phi_{p+1}(s,a) = \frac{\sqrt{2\Re e(a_p)}(s+|a_p|)}{(s+a_p)(s+a_{p+1})} \prod_{j=1}^{p-1} \frac{s-a_j^*}{s+a_j} \tag{5}$$

DOI: 10.1002/jnm

It can be shown that these basis functions are orthonormal with respect to the following inner product ($1 \leqslant m, n \leqslant P$):

$$\langle \Phi_m(s), \Phi_n(s) \rangle_s = \frac{1}{2\pi i} \int_{i\mathbb{R}} \Phi_m(s) \Phi_n^*(s)\, \mathrm{d}s \tag{6}$$

3. TRANSFER FUNCTION IDENTIFICATION

3.1. Levi's estimator

The goal of the frequency domain identification process is to identify the coefficients c_p and $\tilde{c}_p$ in (1) such that the complex fitting error is minimized in a least-squares sense. Levi's linear approximation of this non-linear identification problem can be obtained by solving the following set of equations for all the discrete frequencies $\{s_k\}_{k=0}^{K_s}$ [41]:

$$\arg \min_{c_p, \tilde{c}_p} \sum_{k=0}^{K_s} |N(s_k) - D(s_k) H(s_k)|^2 \tag{7}$$

It is known that Levi's estimator is biased, and therefore it does not guarantee convergence to the true solution of the identification problem [39]. In order to relieve the unbalanced weighting, a Sanathanan–Koerner iteration is applied [11].

3.2. Sanathanan–Koerner iteration

In successive iteration steps ($v = 0, \ldots, V$), the model coefficients $c_p^{(v)}$ and $\tilde{c}_p^{(v)}$ can be updated iteratively by minimizing the Sanathanan–Koerner cost function [11] that uses the previously estimated denominator as an inverse weight to the least-squares equations. In the first step, (8) reduces to (7) since $D^{(-1)}(s) = 1$.

$$\min_{c_p^{(v)}, \tilde{c}_p^{(v)}} \sum_{k=0}^{K_s} \left| \frac{N^{(v)}(s_k)}{D^{(v-1)}(s_k)} - \frac{D^{(v)}(s_k) H(s_k)}{D^{(v-1)}(s_k)} \right|^2 \tag{8}$$

In the classical Sanathanan–Koerner formulation, the coefficients $c_p^{(v)}$ and $\tilde{c}_p^{(v)}$ of $N^{(v)}(s)$ and $D^{(v)}(s)$ are estimated, provided that each equation of the least-squares matrix is given an explicit frequency-dependent weighting $1/D^{(v-1)}(s)$ as shown in (9) and (12). The VF and OVF algorithms perform this weighting in an implicit way, by estimating the coefficients $d_p^{(v)}$ of $N^{(v)}(s)/D^{(v-1)}(s)$ and the coefficients $\tilde{d}_p^{(v)}$ of $D^{(v)}(s)/D^{(v-1)}(s)$ instead, as shown in (11) and (14). It follows that multiplication by an explicit frequency-dependent weighting using the initial poles is equivalent to iterative *pole relocation* without weighting. Unstable poles are flipped into the left half plane by inverting the sign of their real parts:

$$\frac{N^{(v)}(s)}{D^{(v-1)}(s)} = \frac{1}{D^{(v-1)}(s)} \sum_{p=1}^{P} c_p^{(v)} \Phi_p(s, a) \tag{9}$$

$$= \frac{\prod_{p=1}^{P} (s + a_p) \prod_{p=1}^{P-1} (s + z_{p,n}^{(v)})}{\prod_{p=1}^{P} (s + z_{p,d}^{(v-1)}) \prod_{p=1}^{P} (s + a_p)} \tag{10}$$

$$= \sum_{p=1}^{P} d_p^{(v)} \Phi_p(s, z_d^{(v-1)}) \tag{11}$$

$$\frac{D^{(v)}(s)}{D^{(v-1)}(s)} = \frac{1}{D^{(v-1)}(s)} \left(\tilde{c}_0^{(v)} + \sum_{p=1}^{P} \tilde{c}_p^{(v)} \Phi_p(s, a) \right) \tag{12}$$

DOI: 10.1002/jnm

$$= \frac{\prod_{p=1}^{P}(s+a_p)\prod_{p=1}^{P}(s+z_{p,d}^{(v)})}{\prod_{p=1}^{P}(s+z_{p,d}^{(v-1)})\prod_{p=1}^{P}(s+a_p)} \tag{13}$$

$$= \tilde{d}_0^{(v)} + \sum_{p=1}^{P} \tilde{d}_p^{(v)} \Phi_p(s, z_d^{(v-1)}) \tag{14}$$

It was shown in [14] that implicit weighting often provides a better numerical conditioning if the weighting factor $1/D^{(v-1)}(s)$ has a large dynamic variation over the frequency range of interest. The reason is that the conditioning usually improves in successive iterations as the poles are being relocated to better positions. It is also noted that some additional improvements are obtained by scaling each column of the least-squares equations to unity length as in [18]. The convergence of this pole-relocation process is typically obtained in a few iterations provided that the initial set of prescribed poles a is well chosen [7].

3.3. Partial fraction representation

In the final iteration ($v = V$), the transfer function can be defined as the ratio of (11) and (14)

$$R^{(T)}(s) = \frac{\sum_{p=1}^{P} d_p^{(V)} \Phi_p(s, z_d^{(V-1)})}{\tilde{d}_0^{(V)} + \sum_{p=1}^{P} \tilde{d}_p^{(V)} \Phi_p(s, z_d^{(V-1)})} \tag{15}$$

It is clear that (15) can be simplified by cancelling out the relocated basis function poles $z_d^{(V-1)}$. Therefore, it follows that the poles of the transfer function are essentially the zeros of (14) at iteration step V. Based on the minimal state–space realization of $D^{(V)}(s)/D^{(V-1)}(s)$,

$$\begin{aligned} sX(s) &= AX(s) + BU(s) \\ Y(s) &= CX(s) + DU(s) \end{aligned} \tag{16}$$

the poles $z_d^{(V)}$ of the final transfer function $R^{(V)}(s)$ can then be found by solving the eigenvalues of $A - BD^{-1}C$ [42]. More details about the construction of this realization are well described in [14]. Once the poles are known, the transfer function can easily be represented as a pole-residue model, by solving the residues γ_p as a linear approximation problem:

$$\min_{\gamma_p} \sum_{k=0}^{K_s} \left| \sum_{p=1}^{P} \frac{\gamma_p}{s_k + z_{p,d}^{(V)}} - H(s_k) \right|^2 \tag{17}$$

Such a rational function representation can easily be realized as a SPICE equivalent circuit [43, 44].

4. TIME DOMAIN ALGORITHM

4.1. Time domain cost function

It is seen that the nonlinear cost function (2) can be written in terms of an input signal $U(s)$ and the corresponding output signal $Y(s)$, leading to the following equivalent expression:

$$\arg \min_{c_p, \tilde{c}_p} \sum_{k=0}^{K_s} \left| \frac{N(s_k)}{D(s_k)} - \frac{Y(s_k)}{U(s_k)} \right|^2 \tag{18}$$

$$= \arg \min_{c_p, \tilde{c}_p} \sum_{k=0}^{K_s} \left| \frac{N(s_k)U(s_k)}{D(s_k)U(s_k)} - \frac{D(s_k)Y(s_k)}{D(s_k)U(s_k)} \right|^2 \tag{19}$$

DOI: 10.1002/jnm

The time domain identification algorithm minimizes a different nonlinear cost function [36]

$$\arg \min_{c_p,\tilde{c}_p} \sum_{k=0}^{K_s} \left| \frac{N(s_k)}{D(s_k)} U(s_k) - Y(s_k) \right|^2 \tag{20}$$

$$= \arg \min_{c_p,\tilde{c}_p} \sum_{k=0}^{K_s} \left| \frac{N(s_k)U(s_k)}{D(s_k)} - \frac{D(s_k)Y(s_k)}{D(s_k)} \right|^2 \tag{21}$$

Nevertheless, it turns out that (21) is a good choice for time domain identification: if one transforms it to the time domain using the inverse Laplace transformation

$$f(t) = \mathscr{L}^{-1}F(s) = \frac{1}{2\pi i} \int_{\sigma-i\infty}^{\sigma+i\infty} F(s)\mathrm{e}^{st}\,\mathrm{d}s \tag{22}$$

then it becomes clear that this alternative cost function (21) minimizes the difference between the output signal $y(t)$ and the transient response of the model, due to the injected input signal $u(t)$

$$\arg \min_{c_p,\tilde{c}_p} \sum_{k=0}^{K_t} \left| \mathscr{L}^{-1}\left(\frac{N(s)}{D(s)}\right) \star u(t_k) - y(t_k) \right|^2. \tag{23}$$

It is noted that (21) is nonlinear in terms of the model coefficients, and therefore a similar iterative procedure is used as in the frequency domain. In the first iteration step ($v = 0$), a linear approximation of (21) is obtained by assuming that $D(s_k) = 1$ in the denominator. In successive iteration steps ($v = 1, \ldots, V$), the previously estimated denominator is used as an inverse weight to the least-squares equations. This leads to a linear cost function that is similar, but not equivalent, to Levi's (7) and Sanathanan—Koerner's (8) cost function in the frequency domain, since the weighting factor $1/U(s_k)$ is omitted

$$\min_{d_p^{(v)}\tilde{d}_p^{(v)}} \sum_{k=0}^{K_s} \left| \frac{N^{(v)}(s_k)U(s_k)}{D^{(v-1)}(s_k)} - \frac{D^{(v)}(s_k)Y(s_k)}{D^{(v-1)}(s_k)} \right|^2 \tag{24}$$

It can easily be transformed to the time domain by applying the inverse Laplace transform to (24)

$$\min_{d_p^{(v)}\tilde{d}_p^{(v)}} \sum_{k=0}^{K_t} \left| \mathscr{L}^{-1}\left(\frac{N^{(v)}(s)}{D^{(v-1)}(s)}\right) \star u(t_k) - \mathscr{L}^{-1}\left(\frac{D^{(v)}(s)}{D^{(v-1)}(s)}\right) \star y(t_k) \right|^2 \tag{25}$$

If $\phi_p(\mathrm{t}, z_d^{(v-1)})$ denotes the Inverse Laplace Transform of $\Phi_p(s, z_d^{(v-1)})$, then (25) is equivalent to

$$\min_{d_p^{(v)}\tilde{d}_p^{(v)}} \sum_{k=0}^{K_t} \left| \sum_{p=1}^{P} d_p^{(v)}(u \star \phi_p(t_k, z_d^{(v-1)})) - \sum_{p=1}^{P} \tilde{d}_p^{(v)}(y \star \phi_p(t_k, z_d^{(v-1)})) - \tilde{d}_0^{(v)} y(t_k) \right|^2 \tag{26}$$

The fact that no explicit expression is provided for these basis functions is of no consequence, because (26) only needs the convolution of these functions with the input and output signals $u(t)$ and $y(t)$. To compute the filtered signals $u \star \phi_p(\mathrm{t})$ or $y \star \phi_p(\mathrm{t})$, the state–space realization of the orthonormal basis functions Φ_p is simulated with input $u(t)$ or $y(t)$ (using MATLAB's function *lsim*), respectively. The application of (26) to the time domain samples $\{\mathrm{t}_k, u(\mathrm{t}_k), y(\mathrm{t}_k)\}_{k=0}^{K_\mathrm{t}}$ leads to a set of equations which are linear in terms of the coefficients $d_p^{(v)}$ and $\tilde{d}_p^{(v)}$. Using these coefficients and the state–space realization of the basis functions ϕ_p (which is equivalent to the realization of Φ_p), the transfer function (15) can be constructed [15]. Based on (15), the poles $z_d^{(T)}$ of the frequency domain transfer function are found by solving an eigenvalue problem. Once the poles are known, the final transfer function is obtained by solving the coefficients γ_p as a linear problem.

$$\min_{\gamma_p} \sum_{k=0}^{K_t} \left| \sum_{p=1}^{P} \gamma_p \left(u \star \mathrm{e}^{-z_{p,d}^{(T)} t_k} \right) - y(t_k) \right|^2 \tag{27}$$

DOI: 10.1002/jnm

4.2. Orthonormality considerations

In the time domain, the basis functions $\phi_p(t)$ are orthonormal with respect to the time domain inner product ($1 \leqslant m, n \leqslant P$)

$$\langle \phi_m(t), \phi_n(t) \rangle_t = \int_0^\infty \phi_m(t)\phi_n(t)\,\mathrm{d}t \tag{28}$$

Since the Laplace transform is a unitary transformation from the time domain to the frequency domain, this implies that

$$\langle \mathscr{L}\phi_m(t), \mathscr{L}\phi_n(t) \rangle_s = \langle \phi_m(t), \phi_n(t) \rangle_t \tag{29}$$

and

$$\langle \mathscr{L}^{-1}\Phi_m(s), \mathscr{L}^{-1}\Phi_n(s) \rangle_t = \langle \Phi_m(s), \Phi_n(s) \rangle_s \tag{30}$$

It is noted that the basis functions (3)–(5) are obtained by a Gram–Schmidt orthonormalization on a set of partial fractions $\{1/(s+a_p)\}_{p=1}^{P}$, provided that the poles $\{-a_p\}_{p=1}^{P}$ are all stable (i.e. located in the left half of the complex plane). Therefore, a Gram–Schmidt orthonormalization on the set of exponentials $\{\mathrm{e}^{-a_p t}\}_{p=1}^{P}$ in the time domain will yield the inverse Laplace transform of the frequency domain basis functions (3)–(5). It follows that the relevant orthonormal time domain functions $\phi_p(t)$ are obtained by applying the inverse Laplace transform to $\Phi_p(s)$, as in (26) [45].

5. EXAMPLE: POWER BUS STRUCTURE

The time domain identification algorithm is applied to calculate the transfer function of a passive power bus structure [46], based on the transient input and output signal as partially shown in Figure 1. The system is excited with a Gaussian pulse, which is centered at $t = 0.6$ ns, with a width of 0.2 ns and a height of 1 in normalized units. Figure 2 shows the frequency response as a parametric curve in function of the frequency variable s (Smith Chart).

5.1. Numerical results

A suitable set of 100 starting poles is chosen as proposed in [14]

$$\begin{aligned} -a_p &= -\alpha_p + \beta_p i, \quad -a_{p+1} = -\alpha_p - \beta_p i \\ \alpha_p &= \upsilon\beta_{\max} \end{aligned} \tag{31}$$

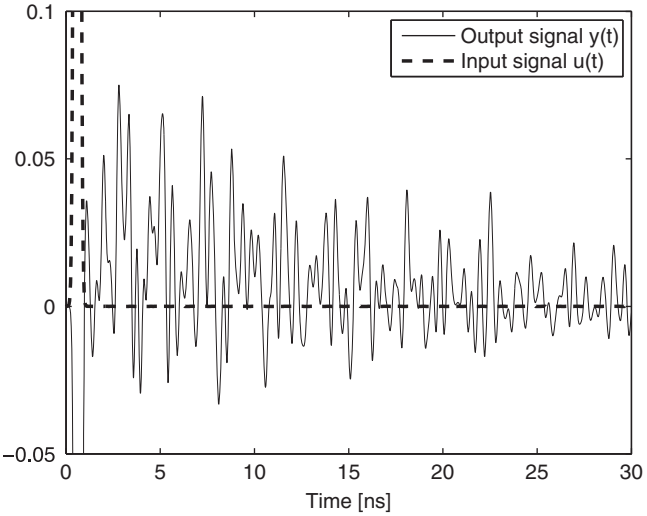

Figure 1. Power bus: Input and output signal of data over interval [0–30 ns].

DOI: 10.1002/jnm

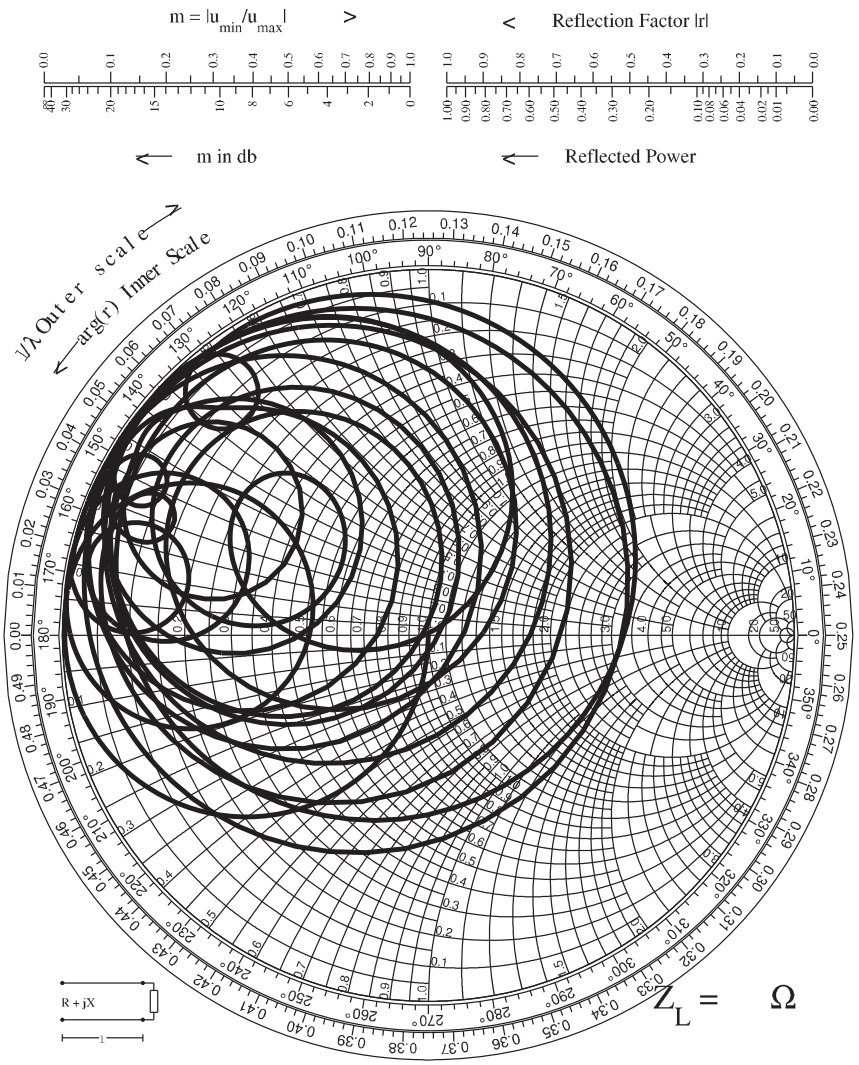

Figure 2. Power bus: Complex frequency response shown in a Smith Chart.

where the imaginary parts β_p are linearly distributed over the frequency range [0–3 GHz], and $\upsilon = 0.01$. The parameter υ is chosen sufficiently small such that the initial poles result in a well-conditioned least-squares matrix. The distribution of the poles over the entire frequency range reduces the probability that poles must be relocated over long distances. It is clear that other prescribed pole-location schemes are also possible, however, they often require more pole-relocation iterations.

Using the set of prescribed poles (31), the weighted linear cost function (25) is solved iteratively, and updated estimates of the model coefficients are obtained. The poles, which define the time domain basis functions, are calculated in each iteration by solving an eigenvalue problem that is based on the estimated coefficients $\tilde{d}_p^{(v)}$. This process is repeated until the poles are converged. In the final iteration, the time domain basis functions are based on the converged set of relocated poles, and the overall transfer function is calculated by minimizing the cost function (27). Table I shows the evolution of the maximum absolute fitting error in successive iteration steps for the time domain VF and OVF algorithms, and it is found that both methods are reliable and lead to satisfactory results in about five iterations.

Owing to the robustness of the orthonormal basis functions, the time domain OVF technique is less sensitive to the initial pole specification than the time domain VF technique presented in [36]. As an example, the real part of the basis function poles is chosen to be non-negligible such that $\upsilon = 0.05$, and the algorithm is allowed to perform only one single iteration. Figure 3 shows

DOI: 10.1002/jnm

that the OVF technique provides a highly accurate approximation of the time domain response, since there is no visible difference between the data and the transient response of the model. As can be seen from Figure 4, the maximal absolute error corresponds to 0.0032. If the same calculations are performed using the VF approach, then the maximal absolute error corresponds to 0.0120, which results in significant time domain discrepancies. As a means of validation, the

Table I. Maximum absolute fitting error of transient response in successive iterations ($\upsilon = 0.01$).

Iteration	VF	OVF
1	0.0030	0.0030
2	0.0020	0.0020
3	0.0011	0.0011
4	0.0010	0.0010
5	0.0008	0.0008

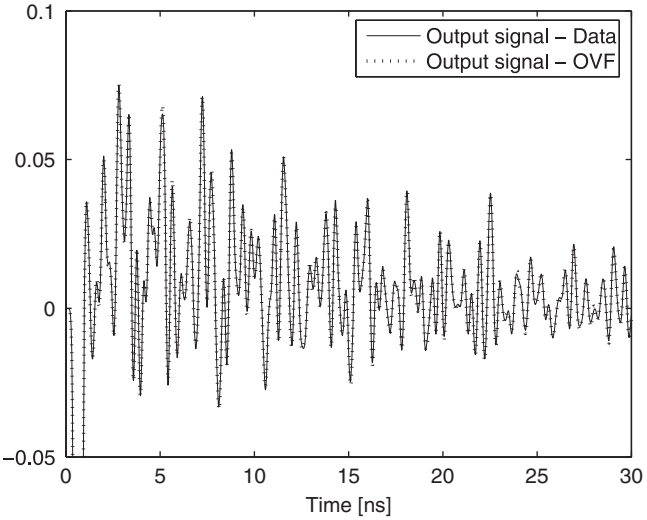

Figure 3. Power bus: Transient response of data and model over interval [0–30 ns].

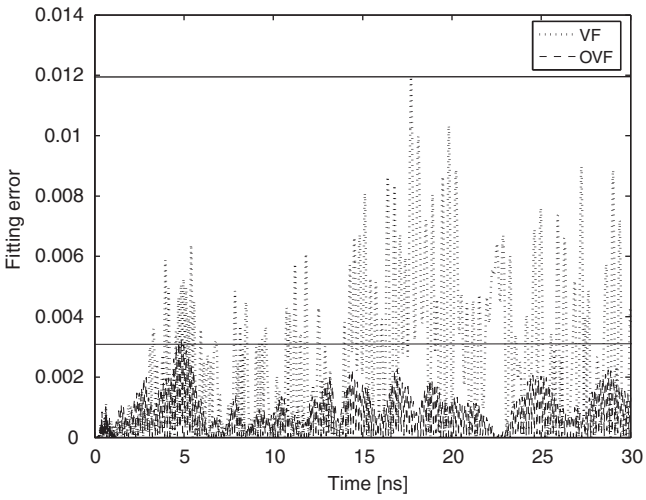

Figure 4. Power bus: Abs. fitting error over interval [0–30 ns]: 1 iter, $\upsilon = 0.05$.

DOI: 10.1002/jnm

OVF-calculated transfer function is simulated in the frequency domain and compared with the reference spectral response. Figures 5 and 6 confirm that an overall good approximation is obtained, both in terms of the magnitude and the phase. Table II illustrates that both approaches eventually converge to better, comparable results if additional iterations are

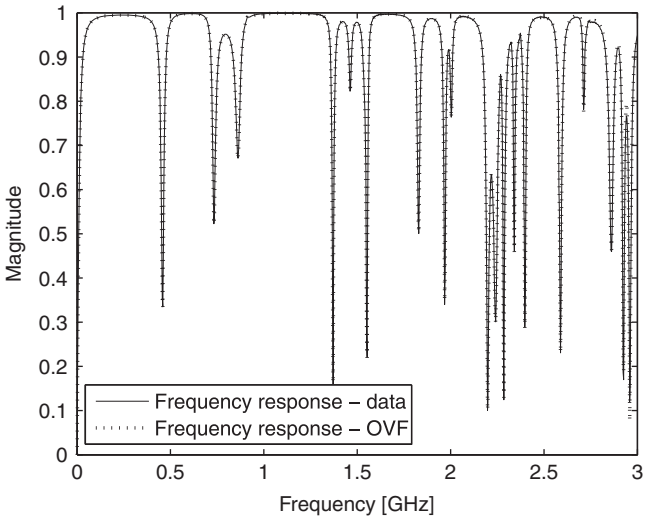

Figure 5. Power bus: Magnitude response of model and reference data.

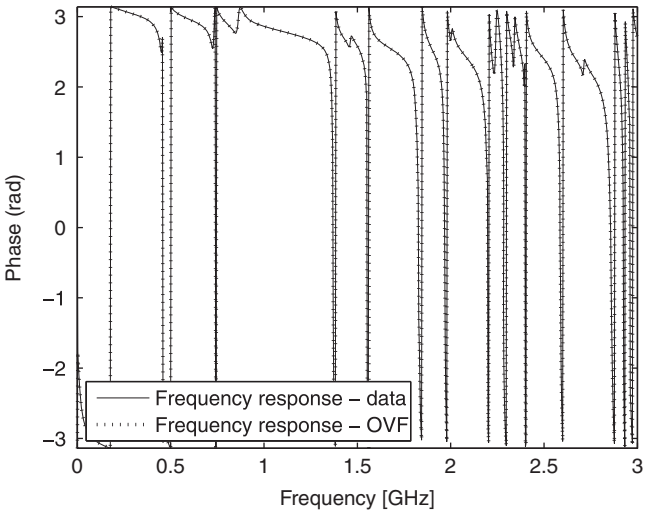

Figure 6. Power bus: Phase response of model and reference data.

Table II. Maximum absolute fitting error of transient response in successive iterations ($\upsilon = 0.05$).

Iteration	VF	OVF
1	0.0120	0.0032
2	0.0035	0.0021
3	0.0022	0.0010
4	0.0013	0.0011
5	0.0009	0.0008

DOI: 10.1002/jnm

performed. This results from the fact that the initial poles (which are selected in a non-optimal way) lead to a poor numerical conditioning in the first iterations. As more iterations are performed, the poles are relocated to a better position, and the accuracy of the fitting model improves gradually. Figure 7 shows the evolution of the maximum absolute fitting error in a single iteration, if the number of starting poles is varied between 50 and 150 using $\upsilon = 0.05$, and it is seen that the improvement holds for an arbitrary number of poles. Figure 8 shows the same results using $\upsilon = 0.01$, and it is found that both algorithms give comparable results. It is seen that OVF is still somewhat more accurate if the number of poles is chosen very high, but this difference has little importance, since it is only observed if the number of poles is chosen much higher than the 'correct' model order. It can be resolved by choosing $\upsilon = 0.001$ a bit smaller than the recommended value, in which case both algorithms give a comparable result, as shown in Figure 9. These figures show that the choice of starting poles is of crucial importance to ensure accuracy of the results in the first iterations. In general, it is found that the OVF approach is numerically more robust towards the initial pole specification and leads to either comparable or better results, depending on the choice of υ.

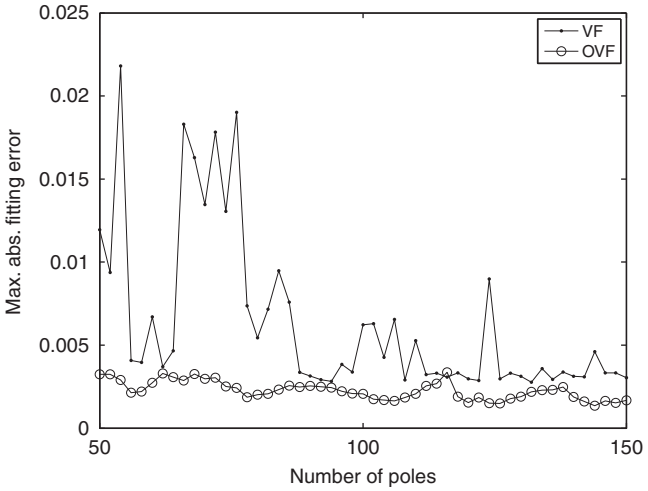

Figure 7. Power bus: Maximum absolute fitting error vs number of starting poles in a single iteration ($\upsilon = 0.05$).

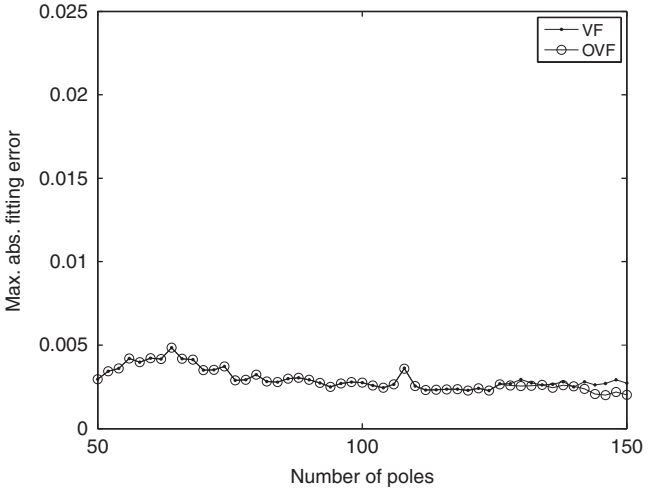

Figure 8. Power bus: Maximum absolute fitting error vs number of starting poles in a single iteration ($\upsilon = 0.01$).

DOI: 10.1002/jnm

6. EXAMPLE: ELLIPTIC LOWPASS FILTER

In this example, the same identification procedure is applied to calculate a macromodel of an elliptic lowpass filter. A commercial full-wave electromagnetic simulator [47] is used to characterize a state–space model of the filter over the frequency range of interest [0–3 GHz]. This filter is excited with a Gaussian pulse that is centered at $t = 0.6$ ns, with a width of 0.2 ns and a height of 1 in normalized units. Based on the output signal of the filter, a 16-pole time domain macromodel is computed by the proposed OVF algorithm. The starting poles are chosen according to the heuristic scheme (31) with $\upsilon = 0.01$, and the poles are relocated in three successive iteration steps. Figure 10 compares the transient response of the filter (solid line) and the response of the OVF model (dotted) up to 100 ns. It is clear that a good agreement is observed. In addition, the frequency response of the filter is compared with the frequency response of the OVF model, and it is seen from Figures 11 and 12 that an excellent agreement is obtained.

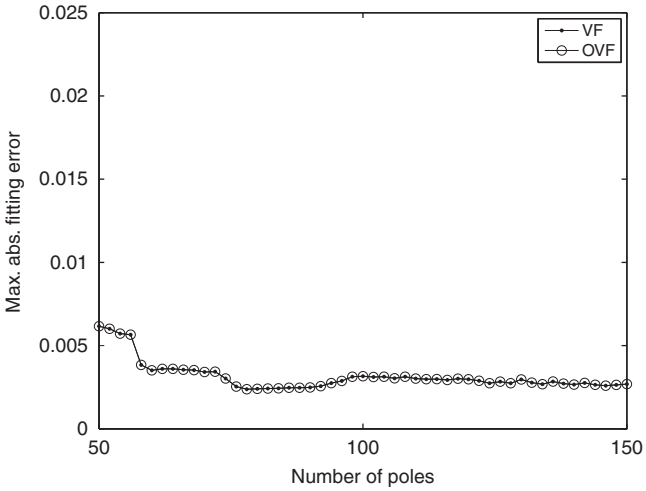

Figure 9. Power bus: Maximum absolute fitting error vs number of starting poles in a single iteration ($\upsilon = 0.001$).

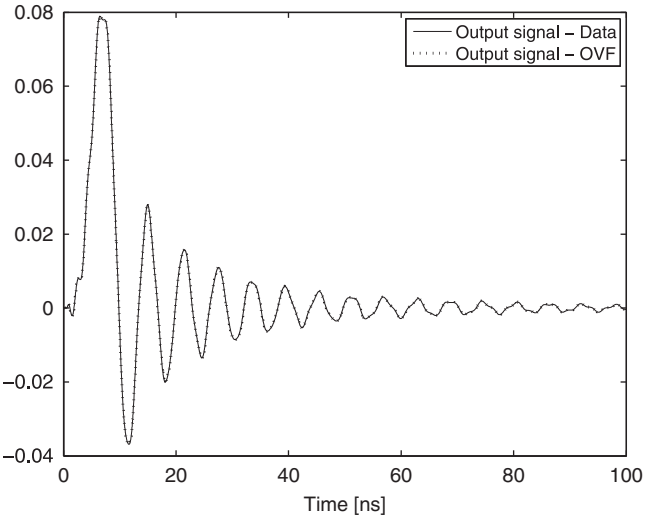

Figure 10. Lowpass filter: Output signal of data over interval [0–100 ns].

DOI: 10.1002/jnm

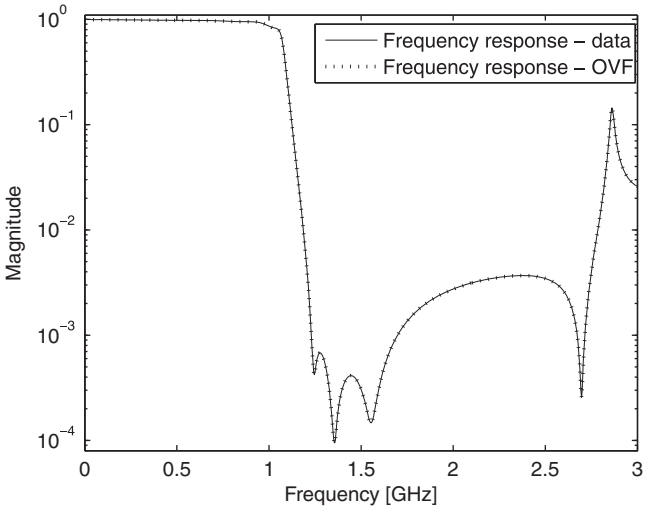

Figure 11. Lowpass filter: Frequency response of model and reference data.

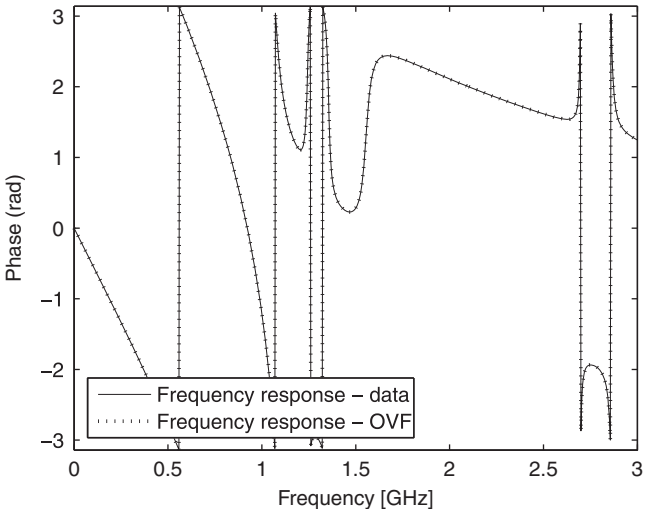

Figure 12. Lowpass filter: Phase response of model and reference data.

As an additional validation test, the frequency response of the filter is subjected to the frequency domain OVF algorithm as reported in [15], and a 16-pole frequency domain macromodel is calculated. Figure 13 visualizes the converged poles of the time domain OVF macromodel ($\times$) and the converged poles of the frequency domain OVF macromodel ($\circ$), and it is seen that both algorithms relocate the starting poles to the same position. This confirms that the time domain identification is reliable and robust.

7. CONCLUSIONS

A time domain generalization of the OVF technique is proposed for accurate broadband macromodeling from transient port responses. It combines the use of a Sanathanan–Koerner iteration and an orthonormal set of basis functions to improve the numerical conditioning. It is shown that the method is less sensitive to the initial pole specification when compared with

DOI: 10.1002/jnm

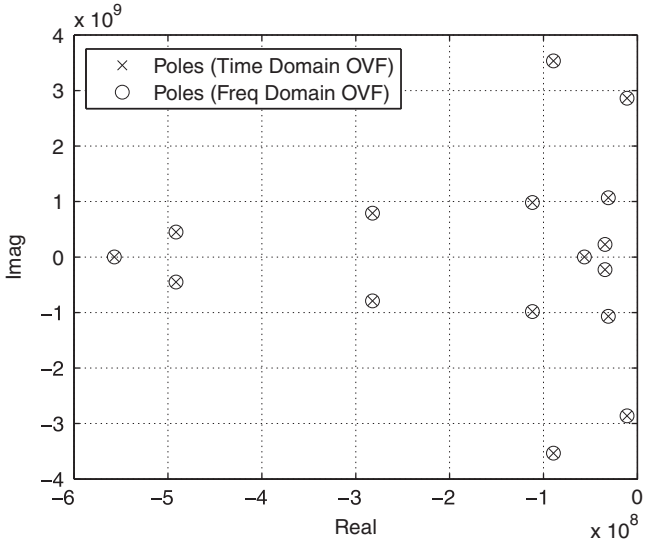

Figure 13. Lowpass filter: Transfer function poles of time domain and frequency domain model.

the standard time domain vector fitting technique. Several examples illustrate the robustness and accuracy of the technique.

ACKNOWLEDGEMENTS

The authors thank Prof. Grivet-Talocia for providing the dataset of the power bus structure. This work was supported by the Research Foundation in Flanders (FWO-Vlaanderen). Dirk Deschrijver is a post-doctoral research fellow of FWO-Vlaanderen.

REFERENCES

1. Li EP, Wei XC, Cangellaris AC, Liu EX, Zhang YJ, D'Amore M, Kim J, Sudo T. Progress review of electromagnetic compatibility analysis technologies for packages, printed circuit boards, and novel interconnects. *IEEE Transactions on Electromagnetic Compatibility* 2010; **52**(2):248–265.
2. Pintelon R, Schoukens J. *System Identification: A Frequency Domain Approach*. IEEE Press: Piscataway, NJ, U.S.A., 2001.
3. Beyene WT, Schutt-Aine JE. Efficient transient simulation of high-speed interconnects characterized by sampled data. *IEEE Transactions on Components, Packaging and Manufacturing Technology—Part B* 1998; **21**(1): 105–114.
4. Gao R, Mekonnen YS, Beyene WT, Schutt-Aine JE. Black-box modeling of passive systems by rational function approximation. *IEEE Transactions on Advanced Packaging* 2005; **28**(2):209–215.
5. Triverio P, Grivet-Talocia S, Nakhla MS, Canavero F, Achar R. Stability, causality and passivity in electrical interconnect models. *IEEE Transactions on Advanced Packaging* 2007; **30**(4):795–808.
6. Lefteriu S, Antoulas AC. A new approach to modeling multiport systems from frequency domain data. *IEEE Transactions on Computer Aided Design of Integrated Circuits and Systems* 2010; **29**(1):14–27.
7. Gustavsen B, Semlyen A. Rational approximation of frequency domain responses by vector fitting. *IEEE Transactions on Power Delivery* 1999; **14**(3): 1052–1061.
8. Gustavsen B. Improving the pole relocating properties of vector fitting. *IEEE Transactions on Power Delivery* 2006; **21**(3):1587–1592.
9. Deschrijver D, Mrozowski M, Dhaene T, De Zutter D. Macromodeling of multiport systems using a fast implementation of the vector fitting method. *IEEE Microwave and Wireless Components Letters* 2008; **18**(6):383–385.
10. Dhaene T, Deschrijver D. Generalised vector fitting algorithm for macromodelling of passive electronic components. *IEE Electronics Letters* 2005; **41**(6):299–300.
11. Sanathanan CK, Koerner J. Transfer function synthesis as a ratio of two complex polynomials. *IEEE Transactions on Automatic Control* 1963; **AC-8**: 56–58.
12. Hendrickx W, Dhaene T. A discussion of rational approximation of frequency domain responses by vector fitting. *IEEE Transactions on Power Systems* 2006; **21**(1):441–443.
13. Hendrickx W, Deschrijver D, Dhaene T. Some remarks on the vector fitting iteration. *Progress in Industrial Mathematics at ECMI 2004*, Mathematics in Industry, vol. 8. Teubner: Stuttgart, 2006; 134–138.
14. Deschrijver D, Gustavsen B, Dhaene T. Advancements in iterative methods for rational

approximation in the frequency domain. *IEEE Transactions on Power Delivery* 2007; **22**(3): 1633–1642.
15. Deschrijver D, Haegeman B, Dhaene T. Orthonormal vector fitting : a robust macromodeling tool for rational approximation of frequency domain responses. *IEEE Transactions on Advanced Packaging* 2007; **30**(2):216–225.
16. Deschrijver D, Dhaene T, Rolain Y. Macromodeling of transfer functions with higher-order pole multiplicities. *Eleventh IEEE Workshop on Signal Propagation on Interconnects* (*SPI 2007*), Genova, Italy, 2007; 53–56.
17. Deschrijver D, Dhaene T. A note on the multiplicity of poles in the vector fitting macromodeling method. *IEEE Transactions on Microwave Theory and Techniques* 2007; **55**(4): 736–741.
18. Gustavsen B. Comments on a comparative study of vector fitting and orthonormal vector fitting techniques for emc applications. *Eighteenth International Zurich Symposium on EMC*, Munich, Germany, 2007; 131–134.
19. Deschrijver D, Dhaene T, De Zutter D. Robust parametric macromodeling using multivariate orthonormal vector fitting. *IEEE Transactions on Microwave Theory and Techniques* 2008; **56**(7):1661–1667.
20. Deschrijver D, Dhaene T. Stability and passivity enforcement of parametric macromodels in time and frequency domain. *IEEE Transactions on Microwave Theory and Techniques* 2008; **56**(11):2435–2441.
21. Triverio P, Grivet-Talocia S, Nakhla MS. A parameterized macromodeling strategy with uniform stability test. *IEEE Transactions on Advanced Packaging* 2009; **32**(1):205–215.
22. Nouri B, Achar R, Nahkla M, Saraswat D. z-Domain orthonormal vector fitting for macromodeling high-speed modules characterized by tabulated data. *Proceedings of the 12th IEEE Workshop on Signal Propagation on Interconnects*, Avignon, France, 2008; 4.
23. Mekonnen YS, Schutt-Aine JE. Broadband macromodeling of sampled frequency data using z-domain vector-fitting method. *Proceedings of the 11th IEEE Workshop on Signal Propagation on Interconnects*, Genova, Italy, 2007; 45–48.
24. Wong N, Lei CU. IIR approximation of FIR filters via discrete-time vector fitting. *IEEE Transactions on Signal Processing* 2008; **56**(3):1296–1302.
25. Mekonnen YS, Schutt-Aine JE. Fast macromodeling technique of sampled time/frequency data using z-domain vector fitting method. *Proceedings of the IEEE Electrical Performance of Electronic Packaging Conference*, Atlanta, GA, USA, 2007; 47–50.
26. Lei CU, Wong N. IIR approximation of FIR filters via discrete-time hybrid-domain vector fitting. *IEEE Signal Processing Letters* 2009; **16**(6):533–536.
27. Kocar I, Mahseredjian J, Olivier G. Weighting method for transient analysis of underground cables. *IEEE Transactions on Power Delivery* 2008; **23**(3):1629–1635.
28. Grivet-Talocia S. Passivity enforcement via perturbation of hamiltonian matrices. *IEEE Transactions on Circuits and Systems I*: *Regular Papers* 2004; **51**(9):1755–1769.
29. Saraswat D, Achar R, Nakhla MS. Global passivity enforcement algorithm for macromodels of interconnect subnetworks characterized by tabulated data. *IEEE Transactions on Very Large Scale Integration Systems* 2005; **13**(7):819–832.
30. Lamecki A, Mrozowski M. Equivalent SPICE circuits with guaranteed passivity from non-passive models. *IEEE Transactions on Microwave Theory and Techniques* 2007; **55**(3):526–532.
31. Grivet-Talocia S, Ubolli A. A comparative study of passivity enforcement schemes for linear lumped macromodels. *IEEE Transactions on Advanced Packaging* 2008; **31**(4):673–683.
32. Dhaene T, Deschrijver D, Stevens N. Efficient algorithm for passivity enforcement of S-parameter based macromodels. *IEEE Transactions on Microwave Theory and Techniques* 2009; **57**(2):415–420.
33. Deschrijver D, Dhaene T. Fast passivity enforcement of S-parameter macromodels by pole perturbation. *IEEE Transactions on Microwave Theory and Techniques* 2009; **57**(3): 620–626.
34. Gao S, Li YS, Zhang MS. An efficient algebraic method for the passivity enforcement of macromodels. *IEEE Transactions on Microwave Theory and Techniques* 2010; **58**(7):1830–1839.
35. Lei CU, Wong N. Efficient linear macromodeling via discrete-time time-domain vector fitting. *Proceedings of the 21st International Conference on VLSI Design*, Hyderabad, India, 2008; 469–474.
36. Grivet-Talocia S. The time-domain vector fitting algorithm for linear macromodeling. *International Journal on Electronics and Communications* (*AEUE*) 2004; **58**:293–295.
37. Haegeman B, Deschrijver D, Dhaene T. Efficient time-domain macromodeling of complex interconnection structures. *Proceedings of the Eurocon 2007 Conference*, Warsaw, Poland, 2007; 85–87.
38. Deschrijver D, Haegeman B, Dhaene T. Robust identification of transient port responses using time domain orthonormal vector fitting. *Proceedings of the 3rd IFAC Symposium on System, Structure and Control*, Foz do Iguacu, Brazil, 2007.
39. Pintelon R, Guillaume P, Rolain Y, Schoukens J, Hamme HV. Parametric identification of transfer functions in the frequency domain—a survey. *IEEE Transactions on Automatic Control* 1994; **39**(11): 2245–2260.
40. Heuberger P, Van Den Hof PMJ, Wahlberg B. *Modelling and Identification with Rational Orthogonal Basis Functions*. Springer: London, 2005.
41. Levi EC. Complex curve fitting. *IEEE Transactions on Automatic Control* 1959; **AC-4**:37–43.
42. Goodwin GC, Graebe SF, Salgado ME. *Control System Design*. Prentice-Hall: NJ, U.S.A., 2001.
43. Antonini G. SPICE equivalent circuits of frequency-domain responses. *IEEE Transactions on Electromagnetic Compatibility* 2003; **45**(3):502–512.
44. Antonini G. Equivalent network synthesis for via holes discontinuities. *IEEE Transactions on Advanced Packaging* 2002; **25**(4):528–536.
45. Bracewell R. *The Fourier Transform & Its Applications* (2nd edn). McGraw-Hill: Reading, NY, U.S.A., 1986.
46. Grivet-Talocia S, Canavero FG, Stievano IS, Maio IA. Circuit extraction via time-domain vector fitting. *Proceedings of the International Symposium on Electromagnetic Compatibility* (*EMC 2004*) 2004; **3**:1005–1010.
47. Sonnet Suites. High frequency electromagnetic software, Syracuse, NY, U.S.A.

AUTHORS' BIOGRAPHIES

D. Deschrijver was born in Tielt, Belgium, on September 26, 1981. He received the Master's (Licentiaat) degree and the PhD degree in Computer Science from the University of Antwerp, Antwerp, Belgium, in 2003 and 2007 respectively. From May to October 2005, he was a Marie Curie Fellow with the Scientific Computing Group, Eindhoven University of Technology, Eindhoven, The Netherlands. He is currently an FWO Post-Doctoral Research Fellow with the Department of Information Technology (INTEC), IBBT, Ghent University, Gent, Belgium. His research interests include robust parametric macromodeling, rational least squares approximation, orthonormal rational functions, system identification, and broadband macromodeling techniques.

T. Dhaene was born in Deinze, Belgium, on June 25, 1966. He received the PhD degree in Electrotechnical Engineering from the University of Ghent, Gent, Belgium, in 1993. From 1989 to 1993, he was a Research Assistant with the Department of Information Technology (INTEC), University of Ghent, where his research was focused on different aspects of full-wave electromagnetic (EM) circuit modeling, transient simulation, and time-domain characterization of high-frequency and highspeed interconnections. From August 1993 to September 2000, he was with the EDA Company Alphabit (later the Hewlett-Packard Company and now part of Agilent Technologies). He was one of the key developers of the planar EM simulator ADS Momentum. From October 2000 to September 2007, he was a Professor with the Department of Mathematics and Computer Science, University of Antwerp, Antwerp, Belgium. Since October 2007, he has been a Full Professor with the INTEC, Ghent University. He has authored or coauthored over 210 peer-reviewed papers and abstracts in international conference proceedings, journals, and books.

DOI: 10.1002/jnm